PAPER

Defect chemistry, redox kinetics, and chemical diffusion of lithium deficient lithium niobate

Jianmin Shi,[*a] **Holger Fritze,**[b] **Günter Borchardt**[c] **and Klaus-Dieter Becker**[a]

High-temperature optical *in situ* spectroscopy was used to investigate the defect absorption, redox kinetics, and chemical diffusion of a lithium deficient (48.4 mol% Li_2O) congruent melting lithium niobate single crystal (c-LN). Under reducing atmospheres of various oxygen activities, a_{O_2}, UV-Vis-NIR spectra measured at 1000 °C are dominated by an absorption band due to free small polarons centered at about 0.93 eV. The polaron band intensity was found to follow a power law of the form $a_{O_2}^m$ with $m = -1/4$. A chemical reduction model involving electrons localized on niobium ions on regular lattice sites can explain the observed defect absorption and its dependence on oxygen activity. The kinetics of reduction and oxidation processes upon oxygen activity jumps and the associated chemical diffusion coefficients are found in close agreement over a range from -0.70 to -14.70 in log a_{O_2}, indicating a reversible redox process. Assuming coupled fluxes of lithium vacancies and free small polarons for the attainment of stoichiometry, the diffusion coefficients of lithium vacancies as well as of lithium ions in the lithium deficient c-LN have been determined at 1000 °C.

Introduction

Lithium niobate ($LiNbO_3$, LN) is one of the most grown and studied electro-optical complex oxide single crystals because of its wide range of technical applications such as frequency conversion, optical waveguide switches, optical modulations, and holographic data storage.[1–3] Lithium niobate-related materials remain under intense investigations on the one hand for improvement and development of industrial applications, especially based on their sensitivity to electromagnetic radiation,[4] on the other hand in regard to fundamental issues of the material, *e.g.* intrinsic and extrinsic defects and their transport properties.[1,3]

Due to the similar ionic radii of Li^+ and Nb^{5+}, ferroelectric LN crystallizes in the $R3c$ structure. This structure possesses a distorted hexagonal close-packed oxygen arrangement with face-sharing octahedral interstices where 2/3 of the octahedral sites are filled by cations along the hexagonal *c*-axis in the sequence of Nb, Li, vacancy, Nb, Li, vacancy, *etc*. The Nb^{5+} ions sit near the center of their octahedra whereas Li^+ ions are more off-center in the octahedral sites.[5]

In the Li_2O–Nb_2O_5 phase diagram, LN exhibits a wide range of existence with the Li_2O content extending from the nominally ideal composition with 50 mole% of Li_2O to a substantial Li-deficiency.[6] LN single crystals grown from a melt containing 48.45 mol% Li_2O yield congruent melting lithium niobate (c-LN) possessing the same Li_2O content as the melt, *i.e.*, a Li_2O-deficiency of 1.55 mol%.[6] To maintain charge neutrality in lithium deficient crystals, a number of niobium ions occupy lithium sites forming the so-called antisite defects, $Nb_{Li}^{••••}$. Lithium vacancies, V'_{Li}, vacant niobium sites, V''''_{Nb}, or defect associates, $(Nb_{Li}^{••••}V'''''_{Nb})'$, may serve as possible charge compensators for niobium antisite ions. Here, the Kröger–Vink notation[7] of point defects has been used. As has been shown theoretically and experimentally, lithium vacancies, V'_{Li}, are the main charge balancers in lithium deficient LN, especially at high temperatures.[3,8] Therefore, the chemical formula of lithium deficient LN can be written in greater detail as $(Li_{Li}^\times)_{1-5x}(Nb_{Li}^{••••})_x(V'_{Li})_{4x}(Nb_{Nb}^\times)O_3$. In the case of c-LN, the *x*-value amounts to 0.010.

Chemical reduction of LN induces a broad region of electronic absorption in the visible and the NIR range. This has been attributed primarily to absorption due to small polarons, *i.e.* to electrons trapped on regular or antisite Nb^{5+} ions (Nb'_{Nb} or $Nb_{Li}^{•••}$) and to their associates, the so-called bipolarons $(Nb'_{Nb}Nb_{Li}^{•••})^{••}$.[9–16] Alternatively, the reduction-induced optical absorption may arise from oxygen vacancy-related color centers.[17–21] However, electron polarons are the presently accepted model based on results obtained from different experimental techniques, *e.g.* EPR[11] and density measurements

[a] *Institute of Physical and Theoretical Chemistry, Technische Universität Braunschweig, Hans-Sommer-Str. 10, 38106 Braunschweig, Germany. E-mail: j.shi@tu-braunschweig.de*
[b] *Institute for Energy Research and Physical Technologies, Technische Universität Clausthal, Am Stollen 19, 38640 Goslar, Germany*
[c] *Institute of Metallurgy, Technische Universität Clausthal, Robert-Koch-Str. 42, 38678 Clausthal-Zellerfeld, Germany*

This journal is © the Owner Societies 2011

Phys. Chem. Chem. Phys., 2011, **13**, 6925–6930 | 6925

by diffraction.[22] For a recent review covering *inter alia* polarons, point defects, and disorder in lithium niobate, see Volk and Wöhlecke.[3]

Three distinct defect-related absorption bands have been identified in lithium niobate. Faust *et al.*[10] assigned the optical absorption band at about 0.99 eV in Zn-doped LN to free small polarons, Nb'_{Nb}, and bands at 1.6 eV and 2.5 eV in reduced c-LN were assigned to bound small polarons $Nb^{\bullet\bullet\bullet}_{Li}$ and bipolarons $(Nb'_{Nb}Nb^{\bullet\bullet\bullet}_{Li})^{\bullet\bullet}$, respectively.[3,9,13,14] Recently, support for the indicated assignment of the optical absorption bands at 1.0, 1.6, and 2.5 eV has also been provided by theoretical calculations.[3,15]

Electronic and ionic transport properties of lithium niobate have been intensively investigated by equilibrium conductivity measurements at high temperatures and various oxygen partial pressures.[23–27] The oxygen activity, a_{O_2}, dependence of electronic conductivity in the low oxygen activity range for example has been observed by several authors[23–26] to follow a power law of the form $(a_{O_2})^m$ with $m = -1/4$. Here, the oxygen activity is defined as $a_{O_2} = p_{O_2}/p^0$ where p_{O_2} represents the oxygen partial pressure and $p^0 = 1$ bar. It is also found that lithium niobate is a good conductor for lithium ions,[17,25–27] whereas recent studies of oxygen diffusion show that anion diffusion is slow in lithium deficient as well as in nearly stoichiometric LN with diffusion coefficients of the order of 10^{-16} m^2 s^{-1}.[28,29] Lithium diffusion coefficients derived from different techniques have been reviewed by Birnie[8] and are found to span a wide range of values from about 10^{-11} to 10^{-13} m^2 s^{-1} at 1000 °C. Obviously, the quantitative aspects of lithium diffusion in LN are not well known, see also the discussion below.

Optical *in situ* spectroscopy at high temperatures has proven a powerful technique to study chemical kinetics in complex oxides.[30–32] Recent investigations of coloration processes in lithium niobate single crystals have demonstrated that the chemical kinetics upon a sudden change in the ambient atmosphere of the sample from pure oxygen to a mixture of argon and hydrogen can be well followed under *in situ* conditions by means of high-temperature optical spectroscopy.[32]

The present paper reports an optical *in situ* study at elevated temperatures on the defect chemistry, redox kinetics, and chemical diffusion in a congruent melting lithium deficient LiNbO$_3$ single crystal, under well controlled experimental conditions. In the kinetic experiments with oxygen activity jumps, emphasis is placed on a_{O_2}-jumps of small size which induce only small perturbations from equilibrium and, thus, are more suitable for the quantitative evaluation of chemical kinetics. The objectives of the present work are to better understand the equilibrium defect structure at high temperatures, to analyze chemical kinetics under well-defined *it situ* conditions, and to determine diffusion coefficients from experimental redox kinetics.

Experimental

An X-cut ((100) plane) congruent lithium niobate single crystal wafer (Crystal Technology, Inc.) was used to prepare an optical absorber of 4×4 mm in size. After polishing its large surfaces the thickness of the absorber was 0.41 mm. The Li$_2$O content in the crystal was determined from the composition dependence of the optical absorption edge in LN.[33] According to the lithium content of 48.4±0.1 mol% Li$_2$O the sample can be characterized as congruent melting (c-LN). It is also found that the Li$_2$O content of the single crystal before and after *in situ* redox treatments at 1000 °C changed by less than 0.1 mol%.

Optical *in situ* measurements at high temperatures were performed using an UV-Vis-NIR high-precision optical spectrometer (Perkin Elmer, Lambda 900) combined with a high-temperature furnace. To minimize the influence of thermal radiation on sample absorbance, the spectrometer was specially designed with monochromators placed between the sample chamber and detectors instead of between light sources and the sample chamber in a conventional setup. The experimental setup is schematically shown in Fig. 1. With this setup, optical
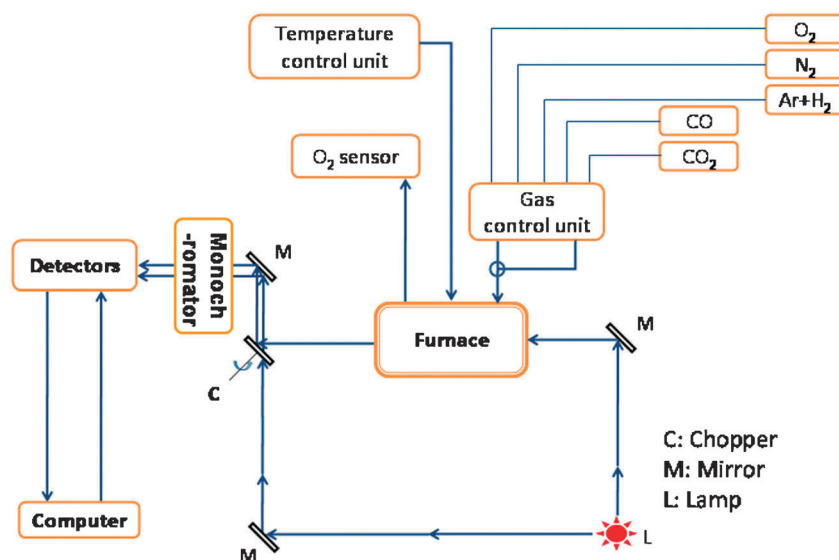

Fig. 1 Schematics of the experimental setup for optical *in situ* measurements.

absorption spectra can be measured from room temperature up to 1300 °C under well-defined oxygen activities using O_2, N_2, $Ar + 5\%H_2$, CO, CO_2 gases or their mixtures. The components of the gas mixture and their flow rates can be set by two gas flow controllers and meters (MKS 647B). For oxygen activity jump relaxation experiments at a fixed temperature, *e.g.* at 1000 °C in this study, the absorber is first equilibrated in the furnace with an atmosphere of well defined oxygen activity and then the sudden change in furnace atmosphere to another a_{O_2} is achieved by switching a 3-way valve in front of the furnace. The time for replacing the sample ambient atmosphere in the furnace was found to be less than 1 min as indicated by an oxygen sensor in the outlet of the furnace.

The quantity determined in the optical experiments is the absorbance A, $A = \log(I_0/I) = \varepsilon cd + A_R = (1000/V_m)\varepsilon[X]d + A_R = \alpha d + A_R$. Here, I_0 and I are the intensities of incoming and transmitted light, respectively. ε and α are the molar and linear absorption coefficients, respectively. c and $[X]$ denote the molar concentration of the absorbing species (mol dm^{-3}) and the number of the indicated species per formula unit of LN, respectively. V_m is the molar volume of the compound (cm^3 mol^{-1}), d represents the absorber thickness, and A_R accounts for surface reflections. It is worth noting that optical spectra at temperatures above 300 °C have been corrected for the thermal radiation emitted by the sample and furnace walls by using separately measured radiation spectra.

Optical relaxation data upon oxygen activity jumps were analyzed using the one dimensional diffusion model, eqn (1),[34] which is considered to be well justified in the present case in view of sample dimensions

$$\frac{A_t - A_\infty}{A_0 - A_\infty} = \sum_0^\infty \frac{8}{(2n+1)^2\pi^2} \exp\left(-\frac{(2n+1)^2\pi^2}{d^2}\tilde{D} \times t\right) \quad (1)$$

Here, A_t denotes the mean absorbance over the thickness d of the absorber at time t after a change in the ambient atmosphere. A_0 and A_∞ are the absorbances at $t = 0$ and $t = \infty$, respectively. $\tilde{D}$ stands for the chemical diffusion coefficient.

Results and discussion

High temperature optical spectra in air

The optical absorption spectra of congruent lithium niobate in air at various temperatures are shown in Fig. 2a for the range from $12\,500$ cm^{-1} to $35\,000$ cm^{-1}. In general, the c-LN absorber remains transparent in the visible range at high temperatures in air. However, the optical absorption edge exhibits a considerable red-shift with increasing temperature. Between room temperature and 1000 °C the shift amounts to about 1.0 eV. The temperature dependence of the absorption edge, E_g, is found to follow a linear relationship $E_g(T) = E_{g,0} + \beta T$ (Fig. 2b) with a temperature coefficient of the optical band gap given by $\beta = -(1.30 \pm 0.01) \times 10^{-3}$ eV K^{-1}. The value extrapolated to zero Kelvin ($E_{g,0}$) is obtained as 4.38 eV which is close to the range of experimental values from about 3.8 to 4.3 eV[35,36] reported for ferroelectric lithium niobate and which is also compatible with theoretical values ranging between 3.47 and 6.53 eV.[37,38]
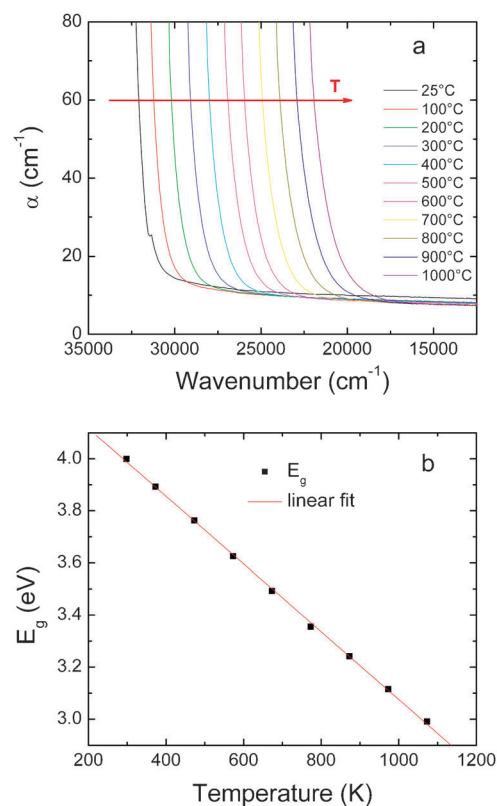

Fig. 2 (a) Temperature dependent optical absorption spectra of c-LN in air, (b) temperature dependence of optical absorption edge.

Defect absorption and defect chemistry

Defect-related equilibrium absorption spectra were collected at 1000 °C after equilibration with furnace atmospheres of various oxygen activities. For clarity reasons, Fig. 3a and b show selected absorption spectra in a reduction run and in an oxidation run, respectively. As seen in Fig. 3a, chemical reduction at 1000 °C produces a broad absorption band at about 7500 cm^{-1} (~ 0.93 eV) whose intensity gradually increases with decreasing oxygen activity. On the other hand, upon re-oxidation, the intensity of this band decreases until it completely disappears in air (Fig. 3b). In view of the small temperature effect on the band position of polaron absorption,[39] this band energy corresponds to the polaron absorption positioned at about 1.0 eV at room temperature which has often been assigned to the optical absorption of free small polarons, Nb'_{Nb}.[3,9,10]
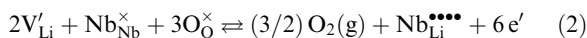
To get insight into the reduction mechanism of c-LN, the dependence of defect concentration on oxygen activity has been extracted from the equilibrium optical spectra. Assuming that the defect concentration, [def], depends on oxygen activity by a power law of the form $[def] = ka_{O_2}^m$, where k is a constant, the parameter m can be determined from a log–log plot of the defect-induced absorbance at fixed wavelength *versus* oxygen activity. Such plots are shown in Fig. 4 for the defect absorbance $A_{def} = \Delta A = A(a_{O_2}) - A(a_{O_2}^*) = (1000/V_m)\varepsilon_{def}[def]d$ at 15 390 cm^{-1} (~ 1.91 eV) and 7500 cm^{-1} (~ 0.93 eV) at 1000 °C, where $a_{O_2}^*$ represents the oxygen activity of synthetic air. From the linear fits of the equilibrium absorption
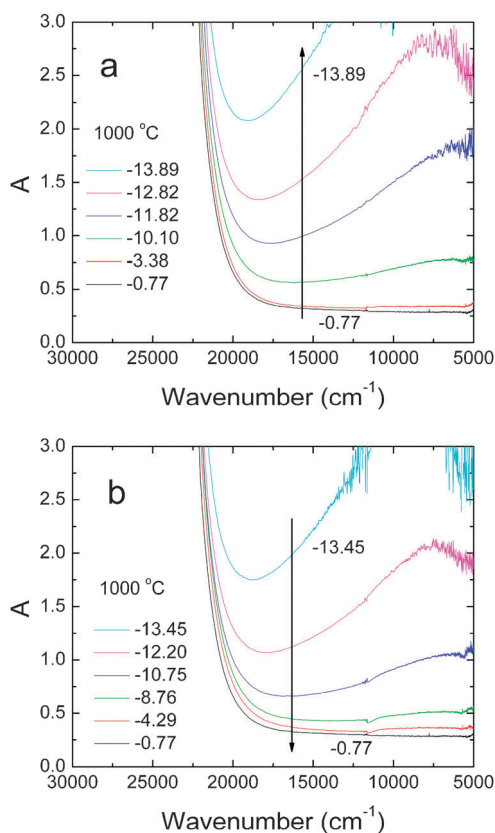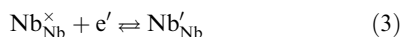
Fig. 3 Equilibrium absorption spectra at 1000 °C for selected oxygen activities showing the change in intensity of the broad defect absorption band, (a) upon reduction starting from $\log a_{O_2} = -0.77$, (b) upon re-oxidation starting from $\log a_{O_2} = -13.45$.

Fig. 4 Oxygen activity dependence of defect absorption $\Delta A = A(a_{O_2}) - A(a_{O_2}^*)$, see text, (a) at 15 390 cm^{-1} ($\sim$1.91 eV) and (b) at 7500 cm^{-1} ($\sim$0.93 eV).

data in the low oxygen activity range ($\log a_{O_2} < -6$) one obtains $m = -(0.24 \pm 0.01)$ for the absorption at 15 390 cm^{-1} and $m = -(0.23 \pm 0.01)$ for the absorption at 7500 cm^{-1}, respectively. Thus, the optical absorbance depends on oxygen activity by obeying a power law with $m = -1/4$ which is in excellent agreement with the oxygen activity dependence of electrical conductivity.[23–26]
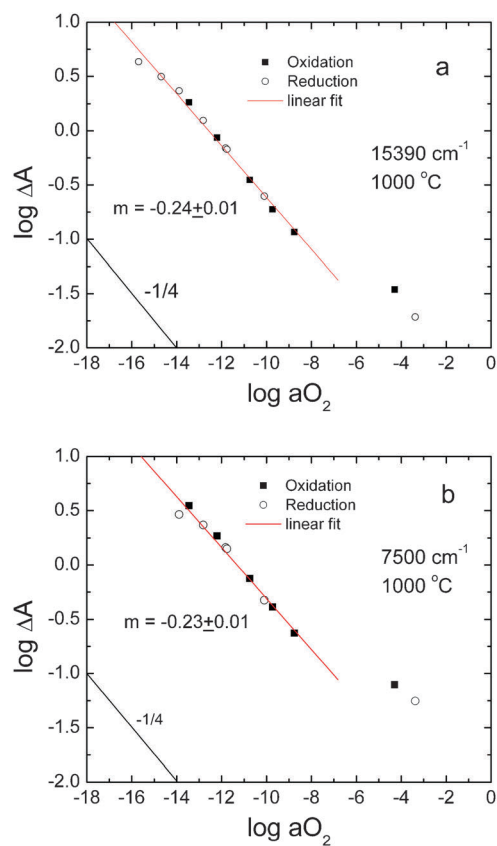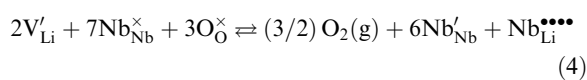
Chemically reduced LN exhibits enhanced electrical conductivity at high temperatures which is correlated with the darkening of the crystal.[11] However, an oxygen vacancy model involving the formation of color centers, $V_O^\bullet$, is not consist with the increase in density of reduced LN and with results from EPR.[11,22] Therefore, a defect model for the reduction of lithium-deficient LN crystals has been proposed involving the formation of niobium antisite ions[3,25,26]

$$2V'_{Li} + Nb^\times_{Nb} + 3O^\times_O \rightleftharpoons (3/2)\,O_2(g) + Nb^{\bullet\bullet\bullet\bullet}_{Li} + 6\,e' \quad (2)$$

At high temperatures, electrons are primarily trapped at niobium ions on regular sites forming free small polarons

$$Nb^\times_{Nb} + e' \rightleftharpoons Nb'_{Nb} \quad (3)$$

which results in an overall reduction reaction of the form

$$2V'_{Li} + 7Nb^\times_{Nb} + 3O^\times_O \rightleftharpoons (3/2)\,O_2(g) + 6Nb'_{Nb} + Nb^{\bullet\bullet\bullet\bullet}_{Li} \quad (4)$$

In the present case of c-LN (48.4 mol% Li$_2$O) with its high concentrations of lithium vacancies ($[V'_{Li}] = 4x \approx 0.04$) and niobium antisite ions ($[Nb^{\bullet\bullet\bullet\bullet}_{Li}] = x \approx 0.01$), it can be assumed that these defect concentrations are not significantly changed by reduction and that, hence, the electroneutrality condition is maintained in the form

$$[V'_{Li}] \approx 4[Nb^{\bullet\bullet\bullet\bullet}_{Li}]. \quad (5)$$

Using the mass action law for eqn (4), one obtains
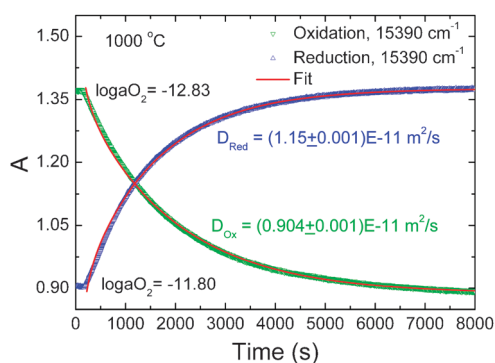
$$[Nb'_{Nb}] = (4K_4)^{1/6}[V'_{Li}]^{1/6}a_{O_2}^{-1/4}, \quad (6)$$

where K_4 is the mass action constant of eqn (4) and where $[V'_{Li}] = 4x \approx 0.04$ for the c-LN crystal used in the present study. Thus, the advantages of the antisite defect model for reduction are twofold. Firstly, it not only foresees the formation of free small polarons, Nb'_{Nb}, for explaining the broad absorption bands at 1000 °C, but it also predicts the $-1/4$ dependence of electronic absorption on oxygen activity as well as that of electrical conductivity. Secondly, the often observed bound polaron and bipolaron absorption at room temperature and at low temperatures in reduced and quenched samples can be easily explained by complementing or replacing eqn (3) with a reaction of electron trapping at niobium antisite ions, $Nb^{\bullet\bullet\bullet}_{Li}$ and further by the association of free and bound electron polarons leading to the formation of bipolarons $(Nb'_{Nb}Nb^{\bullet\bullet\bullet}_{Li})^{\bullet\bullet}$.

Redox kinetics and chemical diffusion

Fig. 5 shows a typical relaxation experiment for monitoring redox processes in c-LN upon sudden changes in oxygen activity. In the graph, optical absorbance is followed at $\sim 15\,390$ cm^{-1} in a relaxation experiment at 1000 °C with $\log a_{O_2}$ changing between -12.80 and -11.83. The data have been fitted according to the diffusion model, eqn (1), and the quality of the fits indicates that the reduction and oxidation processes of c-LN are diffusion-controlled at the present experimental conditions. Chemical diffusion coefficients, $\tilde{D}_{ox}$ and $\tilde{D}_{red}$, obtained from the kinetics of oxidation and reduction are shown in Fig. 6 as a function of oxygen activity. The graph also shows the mean value of the chemical diffusion coefficients and its estimated error, $\log (\tilde{D}/m^2\,s^{-1}) = -10.78 \pm 0.49$. Over the entire range of oxygen activity covered in the present study ($-0.70 < \log a_{O_2} < -15.0$) the chemical diffusion coefficients show no significant dependence on oxygen activity. This finding is compatible with a redox process in c-LN which is primarily dominated by the intrinsic diffusion of lithium vacancies, V'_{Li}, see below. Furthermore, the close agreement of the averaged chemical diffusion coefficients for oxidation, $\log (\tilde{D}_{ox}/m^2\,s^{-1}) = -10.84 \pm 0.44$ and for the
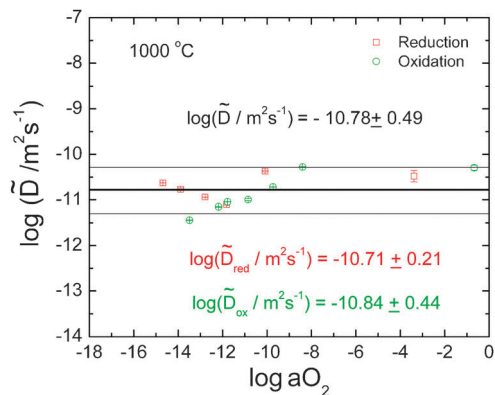
reduction processes, $\log (\tilde{D}_{red}/m^2\,s^{-1}) = -10.71 \pm 0.21$, confirms that the redox processes in c-LN are fully reversible at 1000 °C.

Chemical diffusion in c-LN induced by a sudden change in the oxygen activity of the ambient atmosphere involves the transport of electronic and/or ionic defects. In line with the reduction model, eqn (4), and in view of the immobility of $Nb_{Li}^{\bullet\bullet\bullet\bullet}$ antisite ions, we propose that the fluxes of free small polarons and lithium vacancies are coupled to form a charge-neutral ambipolar diffusion process for the attainment of new crystal stoichiometries. The analysis of ambipolar diffusion of electron polarons and lithium vacancies in c-LN results in the following expression for the chemical diffusion coefficient

$$\tilde{D} = t_e D_{V'_{Li}} + t_i D_e \qquad (7)$$

where t_e and t_i are the transference numbers of the ionic and electronic contribution, respectively.[40] In the reducing atmospheres of our experiments, electrical transport in LN is dominated by electronic conduction, i.e. $t_e \approx 1$.[25,26] Therefore, the chemical diffusion coefficient is practically identical to the Li vacancy diffusion coefficient, $\tilde{D} \approx D_{V'_{Li}} = 1.7 \times 10^{-11}$ m^2 s^{-1}. Provided that Li$^+$ ions diffuse by means of a vacancy mechanism, the diffusion coefficient of Li$^+$ ions can be determined from the relation

$$[Li_{Li}^{\times}]D_{Li^+} = [V'_{Li}]D_{V'_{Li}} \qquad (8)$$

Thus, the diffusion coefficient of lithium ions in the c-LN sample at 1000 °C is obtained from the present optical relaxation measurements as $D_{Li^+} = 0.04\,D_{V'_{Li}} = 6.8 \times 10^{-13}$ m^2 s^{-1}. This value is in excellent agreement with a lithium diffusion coefficient in c-LN of $D_{Li^+} = 7.1 \times 10^{-13}$ m^2 s^{-1} at 1000 °C determined from ^{7}Li NMR relaxation and impedance spectroscopic studies of Heitjans and coworkers.[41,42] It is also in reasonable agreement with an electrical conductivity study of Mehta et al.[26] from which a lithium diffusion coefficient of 1.8×10^{-12} m^2 s^{-1} can be derived at 1000 °C. On the other hand, Ptashnik et al.[43] have reported a lithium tracer diffusion coefficient of 6.8×10^{-12} m^2 s^{-1} at 1000 °C without, however, specifying precisely the composition of the single crystals investigated. A similar value of 6.9×10^{-12} m^2 s^{-1} was also obtained from a temperature-dependent ^{7}Li NMR line-width study of stoichiometric LN.[44] In a theoretical study using density functional theory, Xu et al.[45] determined parameters for the diffusion of lithium vacancies from which a vacancy diffusion coefficient of about 1.3×10^{-12} m^2 s^{-1} can be obtained at 1000 °C. According to eqn (8), from this value a diffusion coefficient of lithium ions of 5.2×10^{-14} m^2 s^{-1} can be calculated for c-LN. Discrepancies similar to the ones observed between the present diffusion coefficients and data from the literature can also be found at 1100 °C, e.g. by comparing results of a diffusion study by Jundt et al.[46] which reported a value of 3×10^{-13} m^2 s^{-1} for lithium diffusion in c-LN at 1100 °C and the abovementioned tracer diffusion study of Ptashnik et al.[43] which yields a lithium tracer diffusion coefficient of 2.5×10^{-11} m^2 s^{-1} at the same temperature.

Fig. 5 Kinetics of typical redox processes at 1000 °C in c-LN upon sudden changes in oxygen activity between $\log a_{O_2} = -12.83$ and $\log a_{O_2} = -11.80$. The solid lines represent the best fits according to the diffusion model, eqn (1).

Fig. 6 Chemical diffusion coefficients for reduction, $\log \tilde{D}_{red}$, and oxidation processes, $\log \tilde{D}_{ox}$, as a function of oxygen activity at 1000 °C. The mean value of the chemical diffusion coefficients, $\log \tilde{D}$, together with its standard estimated error is shown by the solid lines.

Conclusions

Defect chemistry, redox kinetics, and chemical diffusion of a lithium deficient congruent lithium niobate single crystal (c-LN) have been studied by means of optical *in situ* spectroscopy at 1000 °C under various oxygen activities. Optical absorption induced by chemical reduction is dominated by an absorption band due to free small polarons centered at about 0.93 eV. The band intensity is found to follow a power law with a $m = -1/4$ dependence on oxygen activity. A chemical reduction model involving niobium antisite ions successfully accounts for the observed electronic absorption and its oxygen activity dependence. Redox processes in lithium deficient LN upon oxygen activity-jumps are essentially reversible and their kinetics are determined by lithium vacancy diffusion. The chemical diffusion coefficient, the lithium vacancy diffusion coefficient, and the lithium ion diffusion coefficient were determined from the present optical experiments at 1000 °C as 1.7×10^{-11} m^2 s^{-1}, 1.7×10^{-11} m^2 s^{-1}, and 7×10^{-13} m^2 s^{-1}, respectively.

Acknowledgements

References

1 V. Gopalan, V. Dierolf and D. A. Scrymgeour, *Annu. Rev. Mater. Res.*, 2007, **37**, 449.
2 M. E. Lines and A. M. Glass, *Principles and Applications of Ferroelectrics and Related Materials*, Oxford University Press, Oxford, 2001, ch. 16.
3 T. Volk and M. Wöhlecke, *Lithium Niobate, Springer Series in Materials Science*, 2009, vol. 115, ch. 2.
4 M. Kösters, B. Sturman, P. Werheit, D. Haertle and K. Buse, *Nat. Photonics*, 2009, **3**, 510.
5 R. S. Weis and T. K. Gaylord, *Appl. Phys. A: Mater. Sci. Process.*, 1985, **37**, 191.
6 H. M. O'Bryan, P. K. Gallagher and C. D. Braundle, *J. Am. Ceram. Soc.*, 1985, **68**, 493.
7 F. A. Kröger and H. J. Vink, *Solid State Phys.*, 1956, **3**, 273.
8 D. P. Birnie III, *J. Mater. Sci.*, 1993, **28**, 302.
9 O. F. Schirmer, M. Imlau, C. Merschjann and B. Schoke, *J. Phys.: Condens. Matter*, 2009, **21**, 123201.
10 B. Faust, H. Müller and O. F. Schirmer, *Ferroelectrics*, 1994, **153**, 297.
11 D. A. Dutt, F. J. Feigl and G. G. Deleo, *J. Phys. Chem. Solids*, 1990, **51**, 407.
12 H. Jhans, J. M. Honig and C. N. R. Rao, *J. Phys. C: Solid State Phys.*, 1986, **19**, 3649.
13 J. Koppitz, O. F. Schirmer and A. I. Kuznetsov, *Europhys. Lett.*, 1987, **4**, 1055.
14 O. F. Schirmer, O. Thiemann and M. Wöhlecke, *J. Phys. Chem. Solids*, 1991, **52**, 185.
15 H. H. Nahm and C. H. Park, *Phys. Rev. B: Condens. Matter*, 2008, **78**, 184108.
16 C. Merschjann, B. Schoke, D. Conradi, M. Imlau, G. Corradi and K. Polgar, *J. Phys.: Condens. Matter*, 2009, **21**, 015906.
17 S. Bredikhin, S. Scharner, M. Klinger, V. Kveder, B. Red'kin and W. Weppner, *Ionics*, 1997, **3**, 470.
18 T. Suzuki, *J. Cryst. Growth*, 1996, **163**, 403.
19 A. Garcia-Cabanes, J. A. Sanz-Garcia, J. M. Cabrera and F. Agullo-Lopez, *Phys. Rev. B: Condens. Matter*, 1988, **37**, 6085.
20 R. Hodgson and F. Agullo-Lopez, *Solid State Commun.*, 1987, **64**, 965.
21 K. J. Song, *J. Korean Phys. Soc.*, 1993, **26**, 164.
22 N. Iyi, K. Kitamura, F. Izumi, J. K. Yamamoto, T. Hayashi, H. Asano and S. Kimura, *J. Solid State Chem.*, 1992, **101**, 340.
23 G. Bergmann, *Solid State Commun.*, 1968, **6**, 77.
24 P. J. Jorgensen and R. W. Bartlett, *J. Phys. Chem. Solids*, 1969, **30**, 2639.
25 D. M. Smith, Defects and transport in LiNbO$_3$, *Ferroelectrics*, 1983, **50**, 93.
26 A. Mehta, E. K. Chang and D. M. Smith, *J. Mater. Res.*, 1991, **6**, 851.
27 S. Bredikhin, S. Scharner, M. Klinger, V. Kveder, B. Red'kin and W. Weppner, *Solid State Ionics*, 2000, **135**, 737.
28 P. Fielitz, G. Borchardt, R.A. De Souza, M. Martin, M. Masoud and P. Heitjans, *Solid State Sci.*, 2008, **10**, 746.
29 P. Fielitz, O. Schneider, G. Borchardt, A. Weidenfelder, H. Fritze, J. Shi, K. D. Becker, S. Ganschow and R. Bertram, *Solid State Ionics*, 2011, accepted.
30 R. Merkle and J. Maier, *Angew. Chem., Int. Ed.*, 2008, **47**, 3874.
31 J. Shi and K.-D. Becker, *Solid State Ionics*, 2010, **181**, 473.
32 D. Sugak, Y. Zhydachevskii, Y. Sugak, O. Buryy, S. Ubizskii, I. Solskii, M. Schrader and K.-D. Becker, *J. Phys.: Condens. Matter*, 2007, **19**, 086211.
33 L. Kovacs, G. Ruschhaupt, K. Polgar, G. Corradi and M. Wöhlecke, *Appl. Phys. Lett.*, 1997, **70**, 2801.
34 J. Crank, *The Mathematics of Diffusion*, Oxford University Press, 2nd edn, 1975, p. 36.
35 A. Dhar and A. Mansign, *J. Appl. Phys.*, 1990, **66**, 5804.
36 S. Kase and K. Ohi, *Ferroelectrics*, 1974, **8**, 419.
37 C. Thierfelder, S. Sanna, A. Schindlmayr and W. G. Schmidt, *Phys. Status Solidi C*, 2010, **7**, 362.
38 W. G. Schmidt, M. Albrecht, S. Wippermann, S. Blankenburg, E. Rauls, F. Fuchs, C. Rödl, J. Furthmüller and A. Kotani, *Phys. Rev. B: Condens. Matter*, 2006, **74**, 045104.
39 M. Schrader, D. Mienert, T.-S. Oh, H.-I. Yoo and K.-D. Becker, *Solid State Sci.*, 2008, **10**, 768.
40 J. Maier, *Angew. Chem., Int. Ed. Engl.*, 1993, **32**, 528.
41 P. Heitjans, M. Masoud, A. Feldhoff and M. Wilkening, *Faraday Discuss.*, 2007, **134**, 67.
42 D. Bork and P. Heitjans, *J. Phys. Chem. B*, 1998, **102**, 7303.
43 V. B. Ptashnik, T. Yu. Dunaeva and I. V. Myasniko, *Inorg. Mater.(Transl. of Nerog. Mater.)*, 1985, **21**, 1814.
44 T. K. Halstead, *J. Chem. Phys.*, 1970, **53**, 3427.
45 H. Xu, D. Lee, S. B. Sinnott, V. Dierolf, V. Gopalan and S. R. Phillpot, *J. Phys.: Condens. Matter*, 2010, **22**, 135002.
46 D. H. Jundt, M. M. Fejer, R. G. Norwood and P. F. Bordui, *J. Appl. Phys.*, 1992, **72**, 3468.